Tsc3 regulates SPT amino acid choice in *Saccharomyces cerevisiae* by promoting alanine in the sphingolipid pathway[S]

Jihui Ren,* Essa M. Said,[†,§] Aaron Zhong,* Justin Snider,* Christian Ruiz, Christoph Arenz,[†] Lina M. Obeid,[*,††,§§] Geoffrey D. Girnun,[**,††] and Yusuf A. Hannun[1,*,††]**

Department of Medicine,* Department of Pathology,** and Stony Brook Cancer Center,[††] Stony Brook University, Stony Brook, NY; Institute for Chemistry,[†] Humboldt University of Berlin, Berlin, Germany; Department of Chemistry,[§] Faculty of Science, Suez Canal University, Ismailia, Egypt; and Northport Veterans Affairs Medical Center,[§§] Northport, NY

ORCID IDs: 0000-0002-7342-6200 (E.M.S.); 0000-0003-3349-3369 (Y.A.H.)

Abstract The generation of most sphingolipids (SPLs) starts with condensation between serine and an activated long-chain fatty acid catalyzed by serine palmitoyltransferase (SPT). SPT can also use other amino acids to generate small quantities of noncanonical SPLs. The balance between serine-derived and noncanonical SPLs is pivotal; for example, hereditary sensory and autonomic neuropathy type I results from SPT mutations that cause an abnormal accumulation of alanine-derived SPLs. The regulatory mechanism for SPT amino acid selectivity and physiological functions of noncanonical SPLs are unknown. We investigated SPT selection of amino acid substrates by measuring condensation products of serine and alanine in yeast cultures and SPT use of serine and alanine in a *TSC3* knockout model. We identified the Tsc3 subunit of SPT as a regulator of amino acid substrate selectivity by demonstrating its primary function in promoting alanine utilization by SPT and confirmed its requirement for the inhibitory effect of alanine on SPT utilization of serine. Moreover, we observed downstream metabolic consequences to Tsc3 loss: serine influx into the SPL biosynthesis pathway increased through Ypk1-depenedent activation of SPT and ceramide synthases. This Ypk1-dependent activation of serine influx after Tsc3 knockout suggests a potential function for deoxy-sphingoid bases in modulating Ypk1 signaling.— Ren, J., E. M. Said, A. Zhong, J. Snider, C. Ruiz, C. Arenz, L. M. Obeid, G. D. Girnun, and Y. A. Hannun. **Tsc3 regulates SPT amino acid choice in *Saccharomyces cerevisiae* by promoting alanine in the sphingolipid pathway. *J. Lipid Res.* 2018.** 59: **2126–2139.**

Supplementary key words sphingolipids • ceramides • fatty acid • transferase • lipid signaling • lipidomics • mass spectrometry • deoxysphingolipids • Ypk1 • HSAN1 • substrate selectivity • serine palmitoyltransferase

Complex sphingolipids (SPLs) are major components of the lipid bilayer. They may also form lipid rafts and thus participate in signal transduction. Breakdown products and various intermediate SPL metabolites such as long-chain sphingoid bases (LCBs), ceramides, and their phosphorylation derivatives, such as sphingosine-1-phosphate, have been defined as bioactive SPLs because of their role in cellular processes such as cell proliferation, differentiation, apoptosis, heat stress, and inflammatory responses. The production of these SPL precursors is highly regulated, and the impairment of SPL metabolism leads directly to human diseases such as cancer, heart diseases, inflammation, and various forms of neuropathies (1).

De novo biosynthesis of canonical SPLs starts with condensation between serine and palmitoyl-CoA to form 3-ketodihidrosphingosine (3KDS) by serine palmitoyltransferase (SPT) (2). 3KDS is then converted into other LCBs, ceramides, and finally complex SPLs. SPT belongs to a subfamily of pyridoxl 5′-phosphate enzymes known as α-oxoamine synthases, and it exists in all SPL-producing organisms (3). It is composed of a catalytic core and multiple regulatory subunits. The catalytic core is a heterodimer for eukaryotic cells composed of Lcb1/Lcb2 in yeast

This work was supported by National Institutes of Health Grant R35 GM118128 (Y.A.H.). Its contents are solely the responsibility of the authors and do not necessarily represent the official views of the National Institutes of Health.

Manuscript received 2 July 2018 and in revised form 15 August 2018.

Published, JLR Papers in Press, August 28, 2018
DOI https://doi.org/10.1194/jlr.M088195

Abbreviations: CerS, ceramide synthase; dDHS, 1-deoxydihydrosphingosine; DHC, dihydroceramide; DHS, dihydrosphingosine; dPHS, 1-deoxy-phytosphingosine; dSa, 1-deoxysphinganine; d3KDS, 3-keto-1-deoxysphinganine; HSAN1, hereditary sensory neuropathy type 1; LCB, long-chain sphingoid base; PHC, phytoceramide; PHS, phytosphingosine; SD, synthetic defined; SPH, sphingosine; SPL, sphingolipid; SPT, serine palmitoyltransferase; TORC2, target of rapamycin complex 2; YPD, yeast extract, peptone, and glucose; 3KDS, 3-ketodihidrosphingosine.

[1]To whom correspondence should be addressed.
e-mail: yusuf.hannun@stonybrookmedicine.edu

[S] The online version of this article (available at http://www.jlr.org) contains a supplement.

and hLCB1/hLCB2a or hLCB1/hLCB2b in humans (4, 5). The yeast SPT regulatory subunits include Tsc3, Sac1 (a lipid phosphatase), and Orm1/2 (negative regulators). In humans, SPT regulatory subunits include the small subunits SPTssa/SPTssb and ORMDL1/2/3 (6–9). Although SPT small subunits from yeast and mammals, Tsc3 and SPTssa/SPTssb, respectively, share no sequence homology, they are defined as functional homologues because of their proposed common function as SPT activators (7).

In addition to palmitoyl-CoA, SPT can utilize other fatty acyl-CoAs to generate noncanonical SPLs with varying length of the sphingoid backbone. C16 and C20 LCBs that are generated by SPT using myristoyl-CoA and stearoyl-CoA instead of palmitoyl-CoA have been detected in low abundance from various organisms (10–13). It has been suggested that both the SPT catalytic subunit, SPTLC3, and the small regulatory subunit, SPTssb, control SPT acyl-CoA preference (7, 14). Excess SPLs containing C20 LCBs caused by a mutation in mouse SPTssb has been shown to result in neurodegeneration (15).

Likewise, SPT can utilize amino acids other than L-serine, especially L-alanine and L-glycine. This was demonstrated by the detection in various organisms of 1-deoxy- and 1-deoxymethyl- sphingoid bases, which are condensation products of L-alanine or L-glycine with palmitoyl-CoA, respectively (16). They exist in limited amounts in mammalian cells, and their detection is boosted by treating cells with fumonisin B1, the ceramide synthase (CerS) inhibitor (17). The physiologic consequences of imbalance between serine- and nonserine-derived SPLs is demonstrated by hereditary sensory neuropathy type 1 (HSAN1), a human neurological disorder, with most patients carrying point mutations in either hLCB1 or hLCB2a (18–20). It has been proposed that the mutant SPT loses its preference for serine and results in the accumulation of a high level of deoxy- and deoxymethylsphinganine in patients' serum that causes neurotoxicity (21–23). The mechanism behind the amino acid substrate promiscuity associated with these SPT mutants is not known.

To investigate how SPT selects its amino acid substrates, HPLC-ESI-MS/MS methods were developed in this study to directly measure the condensation products between serine/alanine with palmitoyl-CoA from yeast cultures either at the steady state or by monitoring their formation in a real-time manner through a labeling assay using deuterated L-serine or L-alanine. With these methods, Tsc3 was identified as a regulator for SPT amino acid substrate selectivity by primarily promoting alanine utilization by SPT. Knocking out *TSC3* showed the opposite effect on SPT utilization of serine versus alanine with decreased incorporation of alanine and increased influx of serine into the SPL pathway. This study also showed that Ypk1-mediated activation of both SPT and CerS was partially responsible for the increased serine influx in response to *TSC3* knockout. Together, these findings provide important insights into the regulatory mechanism of SPT substrate selectivity and potential physiologic function of deoxy-SPL in regulating Ypk1-signaling pathways.

MATERIALS AND METHODS

Materials

C17-sphingosine (SPH), dihydrosphingosine (DHS), phytosphingosine (PHS), 1-deoxysphinganine (dSa), and C17-DHS were purchased from Avanti Polar Lipids (Alabaster, AL). 3KDS was from Matreya LLC (State College, PA). L-Serine (3,3)-D2 and L-alanine (3,3,3)-D3 were obtained from Cambridge Isotope Laboratories, Inc. (Tewksbury, MA). EDTA free-protease inhibitor cocktail was obtained from Roche (Indianapolis, IN). Protein assay dye was from Bio-Rad (Hercules, CA). All other reagents were from Sigma-Aldrich (St. Louis, MO).

Constructions of yeast strains

All *Saccharomyces cerevisiae* strains used in this study are listed in **Table 1**. *tsc3Δ*::KanMX and *tsc3Δ*::Leu2 strains were generated by first obtaining the PCR product using pFA6a-kanMX6 (24) or pUG73 (25) as template and oligo set 5′~ATAAAGAGTGTAGAAACCGGAAGAACAAAGGTGGAACATATCATAAGGGGAAGAAcggatc cccgggttaattaa~3′ and 5′~TCCCCTTGCCTCCAGCTTATACTATTATTAACCGAATAAGGATATAAATAATCATgaattcgagctcgtttaaac~3′ or 5′~ATAAAGAGTGTAGAAACCGGAAGAACAAAGGTGGAACATATCATAAGGGGAAGAAcagctgaagcttcgtacgc~3′ and 5′~TCCCCTTGCCTCCAGCTTATACTATTATTAACCGAATAAGGATATAAATAATCATgcataggccactagtggatctg~3′ as primers. This was followed by integrating the PCR product into TSC3 genomic loci. The correct integration into the TSC3 loci was confirmed by PCR with genomic DNA from the candidate strains as template and oligo set 5′~CAATAG TAACTCAAAT CATATGC~3′ and 5′~GTGATAAATTTGATCTCATTCC~3′ as primers.

Plasmid construction

The TSC3 open-reading frame plus 300 bp up- and downstream of the TSC3 open-reading-frame DNA region were amplified by PCR from BY4741 genomic DNA with oligo set 5′~cgggatcccgGATTCGATAAATAGAGCACATA~3′ and 5′~gctctagagcATGTGAGAAAGACTTCGGGCT~3′ as primers. The PCR product was ligated into BamH1 and Xba1 sites of pRS315. The construct was confirmed by restriction enzyme digestion and sequence analysis.

Synthesis of 1-deoxy-phytosphingosine and 3-keto-1-deoxysphinganine

See supplemental information online.

Lipid analysis

Lipid extraction and quantification of LCBs by HPLC-ESI-MS/MS was performed as previously described with an Agilent poroshell 120 EC-C18 column (4.6 × 50 mm; 2.7 um particle size) (26). HPLC-ESI-MS/MS quantification of ceramides was performed as previously described with a Peek Scientific C8 column (4.6 × 150 mm; 3 um particle size) (27). Briefly, ~2–4 × 10^8 cells were collected by centrifugation, and 50 pmol C17-SPH (internal standard for LCBs) or C24:1 ceramide (internal standard for dihydroceramide [DHC] and phytoceramide [PHC]) were added to the pellet before lipid extraction. Dried lipids were resuspended in 200 µl mobile-phase B solution (2% formic acid and 1 mM ammonium formate in methanol). An aliquot of 10 µl was subjected to lipid analysis. The mass spectrometer was operated in multiple-reaction monitoring positive-ionization mode. All transitions used are listed in **Table 2**. Data were collected and processed using Xcalibur software. The quantification of sphingoid bases was based on the calibration curve established by plotting the target analyte/internal standard peak-area ratio against concentrations of the target analytes. 3KDS, DHS, PHS, 3-keto-1-deoxysphinganine (d3KDS), 1-deoxydihydrosphingosine (dDHS),

TABLE 1. List of yeast strains used in this study

Strain	Genotype	Source/Reference
BY4741	MATa his3Δ1 leu2Δ0 met15Δ0 ura3Δ0	Dharmacon
BY4742	MATα his3Δ1 leu2Δ0 lys2Δ0 ura3Δ0	Dharmacon
tsc3-1	BY4741 tsc3Δ::KanMX	This study
tsc3-2	BY4742 tsc3Δ::KanMX	This study
pkh1Δ	BY4742 *pkh1Δ*::KanMX	Dharmacon
pkh2Δ	BY4742 *pkh2Δ*::KanMX	Dharmacon
ypk1Δ	BY4742 *ypk1Δ*::KanMX	Dharmacon
ypk2Δ	BY4742 *ypk2Δ*::KanMX	Dharmacon
tsc3Δ pkh1Δ	BY4742 *pkh1Δ*::KanMX *tsc3Δ*::LEU2	This study
tsc3Δ pkh2Δ	BY4742 *pkh2Δ*::KanMX *tsc3Δ*::LEU2	This study
tsc3Δ ypk1Δ	BY4742 *ypk1Δ*::KanMX *tsc3Δ*::LEU2	This study
tsc3Δ ypk2Δ	BY4742 *ypk2Δ*::KanMX *tsc3Δ*::LEU2	This study
orm1Δ orm2Δ	BY4741 *orm1Δ*::KanMX *orm2Δ*::URA3	This study
orm1Δ orm2Δ tsc3Δ	BY4741 *orm1Δ*::KanMX *orm2Δ*::URA3 *tsc3Δ*::LEU2	This study

and 1-deoxy-phytosphingosine (dPHS) were quantitated using calibration curves for each synthetic compound. No synthetic standards are available for the deuterated LCBs, and they were quantitated using calibration curves for their corresponding undeuterated analyte. The relative amount of DHC (d17:0/26:0) and PHC (d17:0/26:0) was expressed as their peak area normalized by the peak area of the internal standard and number of cells (OD) used for each assay.

Yeast microsome membrane preparation

Yeast microsome membrane fractions were prepared by the method adapted from Pinto et al. (10) and as previously described (26). Briefly, yeast cells were collected from the log-phase culture by centrifugation. The pellet was lysed in lysis buffer containing 50 mM potassium phosphate (pH 7.0), 2.5 mM EDTA, 5 mM DTT, and 1× protease inhibitor cocktail and disrupted with beating with 0.5 mm glass beads. The cell lysate was subjected to ultracentrifugation at 100,000 *g* for 1 h at 4°C. The pellet was homogenized with the lysis buffer, and protein concentration was determined with the Bio-Rad protein assay dye.

In vitro SPT activity assay

The in vitro SPT assay was adapted from Ren et al (26). Briefly, 200 μg yeast microsome protein was incubated with 100 μM palmitoyl-CoA, ~0–15.2 mM L-serine (3,3)-D2, and 50 μM pyridoxal phosphate in the presence or absence of 7.6 mM L-alanine in a 200 μl system at 24°C for 30 min. Two milliliters of 0.5 N NH_4OH were added to stop the reaction. After adding 25 pmol C17-SPH (internal standards for MS), lipids were extracted by adding 2.5 ml chloroform methanol (2:1) and then vortexed vigorously. The lower organic phase was washed twice with 5 ml water, dried under nitrogen gas, and reconstituted in 100 μl mobile-phase B. Ten microliters were subjected to HPLC-ESI-MS/MS analysis to measure the incorporation of L-serine (3,3)-D2 into D2-3KDS. SPT velocity was measured by the amount of 3KDS products generated per minute per milligram of microsome proteins.

Measurement of incorporation of deuterated L-serine or L-alanine into the SPL pathway

Yeasts were cultured to late-log phase at 24°C overnight in synthetic defined (SD) medium supplemented with 2% glucose and amino acids required for the auxotrophic marker. Cells were collected by centrifugation and resuspended in a fresh medium at a density of ~1 OD600 (2×10^7 cells/ml) and cultured for another 30 min. Approximately 7.6 mM L-serine (3,3)-D2 or L-alanine (3,3,3)-D3 were added to the culture. Approximately 2–4 × 10^8 cells were collected at each time point. Cells were kept on ice with 5% trichloroacetic acid for at least 15 min before centrifugation at 3,000 *g* for 5 min. The cell pellets were washed twice with water before being subjected to lipid extraction. D2-3KDS and D2-DHS were quantified with HPLC-ESI-MS/MS to measure the in vivo SPT activity toward serine. D3-d3KDS and D3-dSa were measured to monitor the in vivo SPT activity toward alanine.

In vivo labeling assay with C17-DHS to study CerS activity

Yeasts were cultured to late-log phase before collection and resuspension at ~1 OD600 (2×10^7 cells/ml). C17-DHS was added to the culture (at 10 μM), and ~2–4 × 10^8 cells were collected at each time point (0, 15, 30, and 60 min). Cells were kept on ice in the presence of 5% trichloroacetic acid for at least 15 min

TABLE 2. MS/MS parameters used for the listed analytes

Analyte	Elemental Composition	Parental (M + H) (*m/z*)	Product (M + H) (*m/z*)	Collision Energy (eV)
3KDS	$C_{18}H_{37}NO_2$	300.2	270.3	19
DHS	$C_{18}H_{39}NO_2$	302.3	60.1	15
PHS	$C_{18}H_{39}NO_3$	318.3	300.3	14
D2-3KDS	$C_{18}H_{35}D_2NO_2$	302.2	270.3	19
d3KDS	$C_{18}H_{37}NO$	284.3	81.1	20
dDHS	$C_{18}H_{39}NO$	286.3	268.3	16
dPHS	$C_{18}H_{39}NO_2$	302.3	284.3	17
D3-d3KDS	$C_{18}H_{34}D_3NO$	287.3	84.1	20
C17-DHS	$C_{17}H_{37}NO_2$	288.3	60.1	17
C17-PHS	$C_{17}H_{37}NO_3$	304.3	286.3	14
DHC (d17:0/26:0)	$C_{43}H_{87}NO_3$	666.6	648.5	17
PHC (d17:0/26:0)	$C_{43}H_{87}NO_4$	682.5	268.2	25
DHC (d18:0/26:0)	$C_{44}H_{89}NO_3$	680.5	662.5	17
PHC (d18:0/26:0)	$C_{44}H_{89}NO_4$	696.5	282.2	30
C17-SPH	$C_{17}H_{35}NO_2$	286.2	268.3	17
C24:1Cer	$C_{42}H_{49}NO_3$	648.6	264.8	26

before collecting with centrifugation. After washing twice with water, the cell pellets were collected and subjected to lipid extraction. HPLC-ESI-MS/MS was used to quantify the amount of C17-DHC, C17-PHS, and C17-PHC converted from C17-DHS labeling.

Amino acid analysis with GC/MS

Yeast cells (5 OD) cultured in either SD medium or yeast extract, peptone, and glucose (YPD) were collected and washed twice with water. Amino acid extraction was performed by boiling the yeast pellets in 1 ml water for 15 min followed by centrifugation and collecting the supernatant. Three hundred microliters of the supernatant were evaporated and, along with 5 nmol adonitol (internal standard), treated with 50 µl Mox reagent (2% methoxyamine-hydrogen chloride in pyridine) at 42°C for 1 h before derivatization with 100 µl bis(trimethylsilyl)trifluoroacetamide containing 1% trimethylchlorosilane at 75°C for 1 h. Two microliters of the sample were loaded into an Agilent GS/MS system (7890B GC and 5977A MSD) with an HP-5MS stationary column. Standard curves for all the amino acids tested were generated by the same aforementioned method, with the known quantity ranging from 1 to 100 ng. The amino acid content from the samples was quantified by calculating with the standard curves.

RESULTS

Detection of deoxy-sphingoid bases in yeast *S. cerevisiae* using HPLC-ESI-MS/MS

To study the utilization of serine versus alanine by SPT into the SPL pathway, it is important to be able to measure the SPL products generated by each amino acid. Serine is incorporated into the SPL pathway by first forming 3KDS catalyzed by SPT (2). 3KDS is then converted to DHS, which is also called sphinganine, by yeast 3KDS reductase Tsc10 (28). DHS is further hydroxylated by the sphinganine C4-hydrxylase, Sur2, to form PHS (29). Although PHS is the major LCB species in yeast, both DHS and 3KDS have also been detected (26). Alanine can also be utilized by SPT to form d3KDS, which is further converted into dSa and dPHS using Tsc10 and Sur2, respectively. The detection of dSa, which is also referred to as dDHS (both terms are used interchangeably in this study to be consistent with the current literature), has been reported in multiple organisms such as the marine organism *Spisula polynyma* and fungus *Fusarium* (30, 31). The detection of dSa in mammalian cells was facilitated by the use of fumonisin B1, the CerS inhibitor that causes accumulation of dSa (17). The detection of the free forms of d3KDS and dPHS has not been reported. Detecting these compounds, especially d3KDS, is important in studying SPT activity because it is the direct product generated by SPT. To detect the existence of these two molecules in yeast using HPLC-ESI-MS/MS, the standards of both compounds were first synthesized. These synthesized compounds were used to determine their retention time on the HPLC column and the specific signature fragmentation pattern under positive-ion-mode ESI-MS/MS. d3KDS was detected with a parent *m/z* at 284.3 and a transition at 284.3 > 81.1 (**Fig. 1A**), and dPHS was detected with a parent *m/z* at 302.3 and a transition at 302.3 > 284.3 (although this transition can also detect DHS, they can be well separated on the HPLC column with a different retention time) (Fig. 1C). There was complete separation between d3KDS and dPHS on the HPLC column (~3 min apart). The detection of dSa is also shown in Fig. 1B with a transition at 286.3 > 268.3. Although dSa and d3KDS are very close together on the HPLC (which is not surprising considering the closeness of the two structures), d3KDS was consistently eluted before the dSa peak. After the HPLC-ESI-MS/MS detection parameters were determined with the pure compound, their existence in yeast was evaluated. Whole-cell lipid extract from three different yeast strains that are commonly used in research laboratories were analyzed for the existence of free LCBs and deoxy-LCBs (Fig. 1D). We made the following observations: *1*) all three LCB products formed by SPT (3KDS), Tsc10 (DHS), and Sur2 (PHS) with either serine or alanine as substrates were detected; *2*) consistent with previous reports, PHS was the major serine-derived LCB species in yeast; *3*) in contrast, dPHS was a minor alanine-derived species compared with d3KDS and dSa; *4*) both 3KDS and d3KDS were observed at comparable levels as DHS and dDHS; and *5*) serine-derived DHS and alanine-derived dSa exist at comparable levels. This is different than mammalian cells, where the detection of dSa is only boosted by the addition of CerS inhibitors. This is also surprising because it differs from the common belief that dSa is toxic for cell growth and only exists in excess amount under pathological conditions such as HSAN1.

These results were obtained in yeast that were cultured in SD medium supplemented with amino acids that are only necessary for the auxotrophic growth. To further confirm the detection of free deoxy-sphingoid bases, we used YPD, another commonly used medium, to culture the same yeast strains and used the lipid extracts for HPLC-ESI-MS/MS analysis (Fig. 1E). The deoxy-sphingoid bases were still detected under this culture condition, although they became the minor species compared with serine-derived sphingoid bases. It should be noted that dPHS was not detected under these conditions. Thus, with this method we were able to confirm the existence of deoxy-LCB species in yeast and, compared with serine-derived LCBs, their levels varied under different culture conditions/media. We reasoned this difference in deoxy-LCB levels might stem from the distinctive cellular amino acid pool caused by the different culture medium. To test this hypothesis, we measured the cellular level of free amino acids, including alanine, serine, aspartate, glutamine, glycine, leucine, isoleucine, methionine, valine, and cysteine using GC/MS. The most marked change we observed was the level of free cellular alanine, with an ~8-fold increase for BY4741 cultured in the SD compared with YPD culture. For the two other strains, JK93dα and W303, the change was ~4-fold (Fig. 1F). At the same time, no obvious differences in cellular serine levels between the YPD and SD cultures were observed for any of the three strains (Fig. 1G). The molar ratio between alanine and serine in the YPD culture was ~3, and this ratio rose to ~21 in the SD culture for BY4741. For the other two strains tested, the molar ratio between cellular

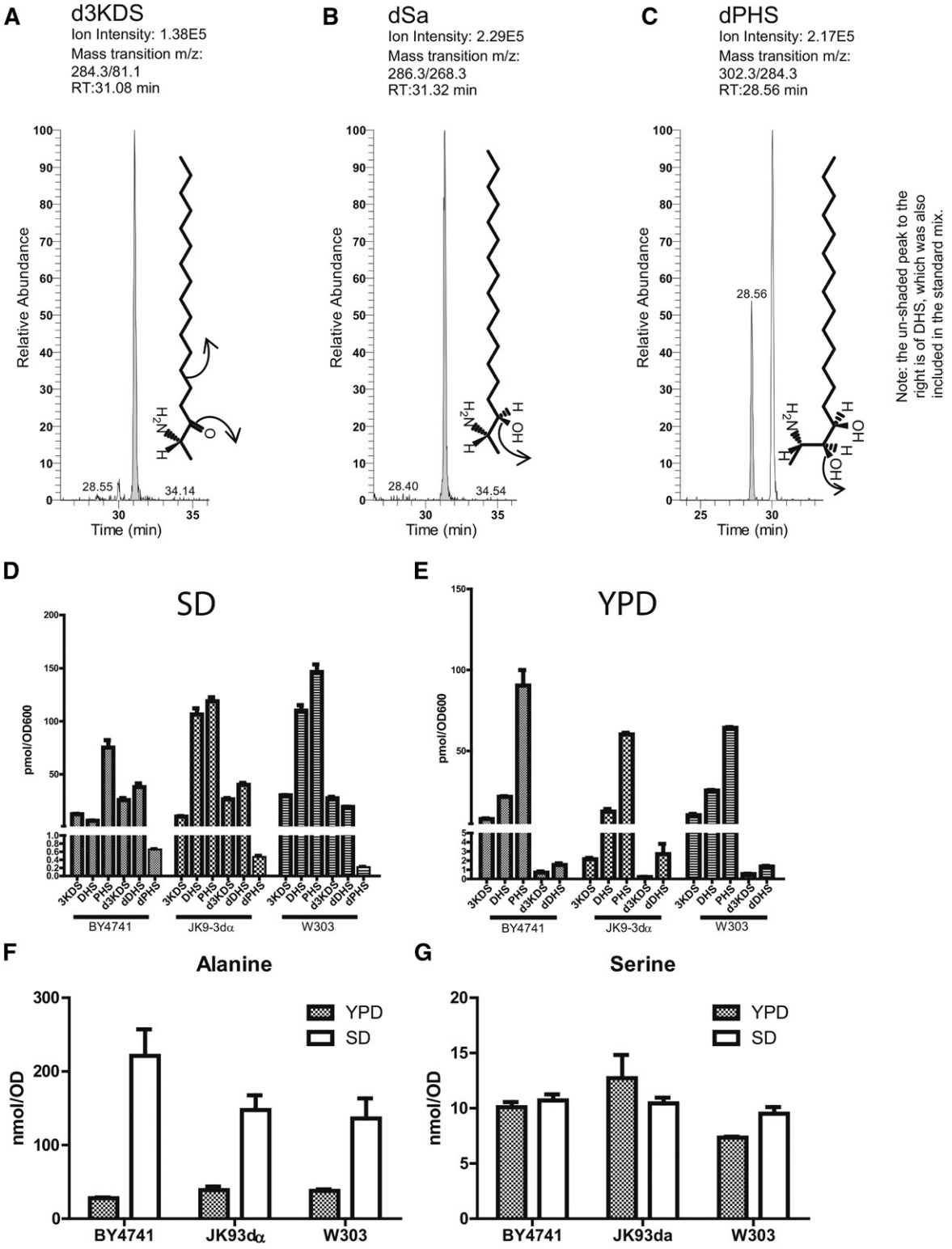

Fig. 1. Detection of d3KDS, dDHS, and dPHS using HPLC-ESI-MS/MS. HPLC separation of 0.625 pmol d3KDS (A), dDHS (B), and dPHS (C) followed by positive-ion-mode ESI-MS/MS. Ion intensities, RT, and parent/product ion pairs are shown in the legends to the right of the SRM peaks. Also shown are the chemical structures of each compound and their fragmentation scheme. Free LCBs from indicated yeast strains cultured in SD (D) or YPD (E) medium at 24°C to the log phase were analyzed. Amino acids were also extracted from these cultures, and the levels of alanine (F) and serine (G) are shown. Values shown on the bar graph are the means of three independent experiments, with the error bars representing standard deviations. RT, retention time; SRM, selected reaction monitoring.

alanine and serine increased from ∼4 in the YPD culture to ∼14 in the SD culture. This correlation between the ratio of cellular free alanine and serine with the deoxy-LCB levels suggests substrate availability might play a key role in determining the balance between serine- and alanine-derived SPLs.

Level of free LCBs changes in *tsc3Δ* and *orm1Δorm2Δ* mutants

To study the regulation of the amino acid selectivity of SPT, we started by evaluating known SPT regulators and their effects on the balance between free LCBs generated from serine or alanine. Tsc3 is a small subunit of the SPT complex, and it has been reported as a positive regulator of SPT (6). Orm1 and Orm2 are redundant homologous transmembrane proteins that reside in the endoplasmic reticulum (8). Orm proteins negatively regulate SPL synthesis by binding to and inhibiting SPT activity (9). SPT activity can be derepressed through the inactivation of Orm proteins via their phosphorylation. Whole-cell lipid extracts from WT, *tsc3Δ*, and *orm1Δorm2Δ* were analyzed for their free LCB contents (**Fig. 2A**). Both mutants showed different LCB levels from WT strains. Both serine- and alanine-derived LCBs were increased in *orm1Δorm2Δ*, with the most marked increases in serine-derived LCBs, including levels of 3KDS, DHS, and PHS. The increase in alanine-derived deoxy-LCBs was most obvious at the dPHS level, whereas the levels of d3KDS and dSa were mildly reduced compared with the WT strain. This accumulation of LCBs in *orm1Δorm2Δ* is consistent with their proposed role of being general negative regulators of SPT.

Because Tsc3 was proposed to be an SPT activator, we expected to observe the opposite effect of *TSC3* deletion on the free LCB levels. In fact, *tsc3Δ* showed markedly decreased levels of all three deoxy-LCBs, including d3KDS, dDHS, and dPHS, compared with WT (Fig. 2A). dPHS in *tsc3Δ* was even below the linear detection range. Surprisingly, instead of decreased serine-derived LCBs, increased levels of 3KDS and DHS were observed in *tsc3Δ* compared with WT strains (Fig. 2A). This increase did not carry on to the PHS level (Fig. 2A). The increased 3KDS and decreased d3KDS levels in *tsc3Δ* yeasts suggest

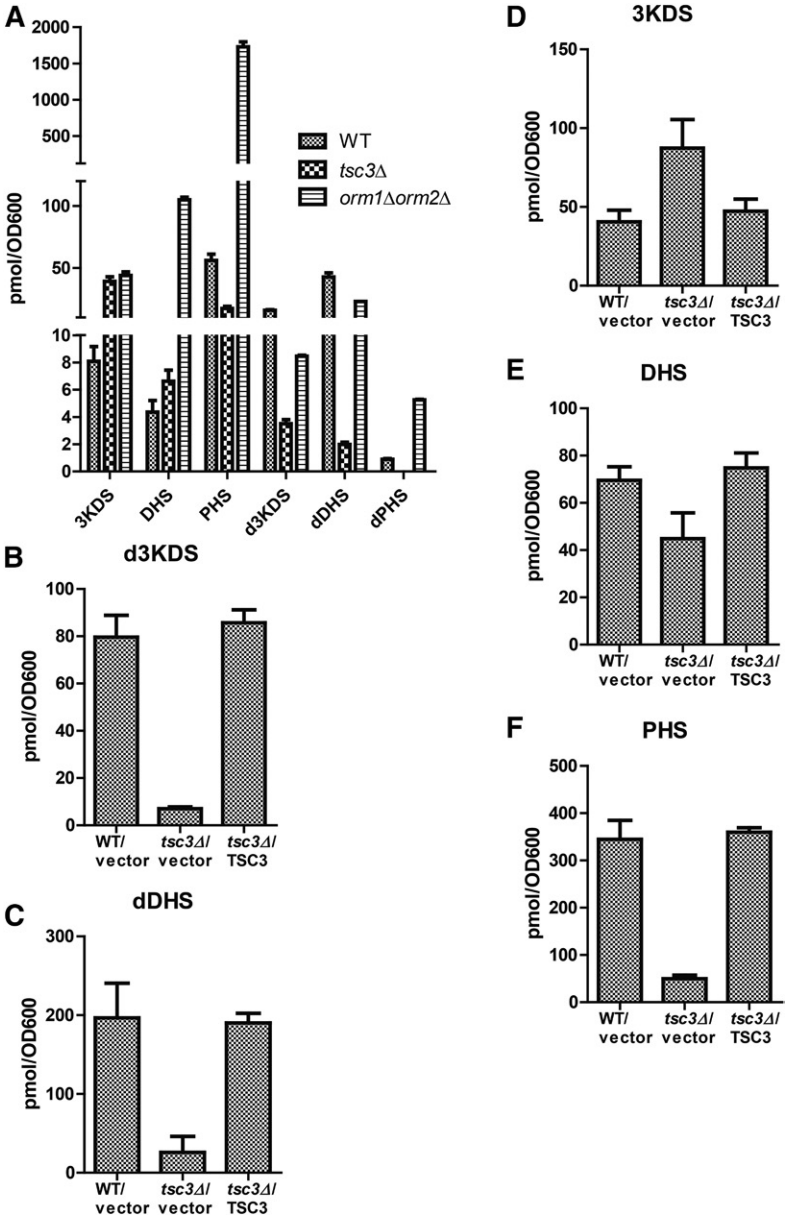

Fig. 2. Increased 3KDS and decreased d3KDS in *tsc3Δ* yeast. A: Measurement of LCB levels in WT, *tsc3Δ*, and *orm1Δorm2Δ* yeast strains. Yeast cells were cultured in SD medium to the late-log phase at 24°C. Cells were collected and subjected to lipid extraction followed by HPLC-ESI-MS/MS. B–F: Measurement of the levels of the indicated LCBs in WT, *tsc3Δ*, and *tsc3Δ* transformed with the WT *TSC3* gene (*tsc3Δ/TSC3*). Cells were cultured in SD-leucine to the late-log phase before lipid extraction. The lipid measurement for each LCB species is represented as the mean from three independent cultures, with the standard deviation calculated using GraphPad Prism 5.

that Tsc3 has opposite effects on serine and alanine incorporation into the SPL pathway. To confirm that *TSC3* is the sole gene responsible for the lipid profile change seen in *tsc3Δ*, we performed lipid analysis to quantify both serine- and alanine-derived free LCBs in *tsc3Δ* strains transformed with a yeast plasmid containing the WT *TSC3* gene under its native promotor (Fig. 2B–F). Under this culture condition, the accumulation of serine-derived free LCBs was only evident at the 3KDS level. All three major changes in free LCB profiles in *tsc3Δ* compared with WT yeast, including 3KDS accumulation, decreased deoxy-LCBs, and decreased PHS levels, were rescued in this strain with the introduction of the WT *TSC3* gene back to the knockout mutant. These results demonstrate that the changes in LCBs seen in *tsc3Δ* were due to the loss of *TSC3*.

Tsc3 controls amino acid selectivity of SPT by promoting alanine incorporation into the SPL biosynthetic pathway

The accumulation of 3KDS but reduction of d3KDS observed in *tsc3Δ* cells by measuring the steady-state level of free sphingoid bases strongly suggests an opposite role of Tsc3 in controlling SPT serine/alanine selectivity in yeast. However, the steady-state measurement of LCBs does not necessarily reflect the SPT activity because this measurement shows the cumulative effects of multiple metabolic processes. To monitor the incorporation of amino acids into the SPL pathway in real time, a labeling assay was developed using deuterated serine and alanine as substrates (**Fig. 3A**, B). L-Serine (3,3)-D2 or L-alanine (3,3,3)-D3 (7.6 mM, respectively) was added to the SD medium, which does not normally contain serine or alanine, and the formation of deuterated 3KDS or d3KDS products was monitored

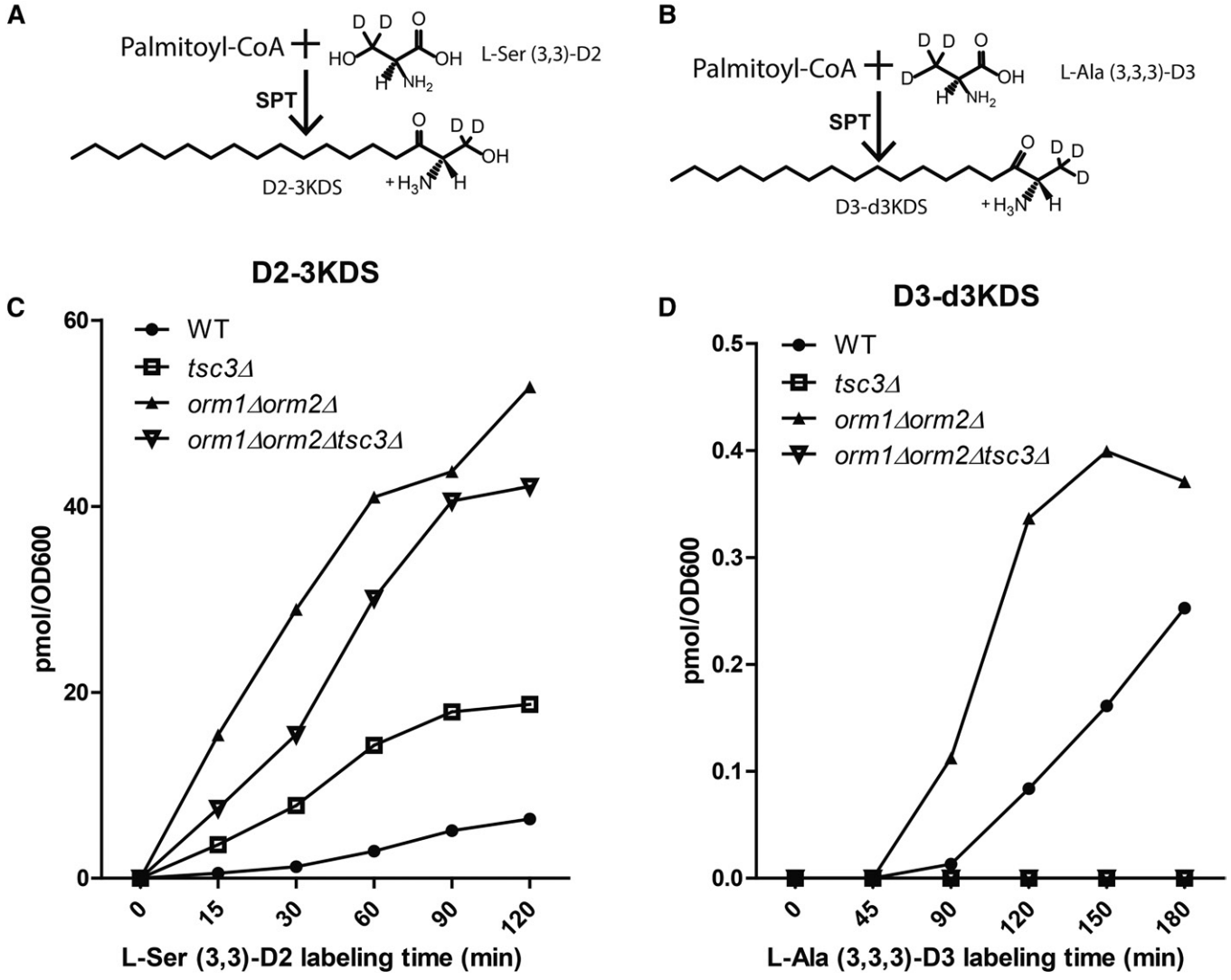

Fig. 3. Increased L-serine (3,3)-D2 and decreased L-alanine (3,3,3)-D3 utilization by SPT in *tsc3Δ* yeast. A, B: Chemical structures of deuterated L-serine, L-serine (3,3)-D2, and deuterated L-alanine, L-alanine (3,3,3)-D3, and their SPT products D2-3KDS and D3-d3KDS. C, D: Increased L-serine (3,3)-D2 incorporation into D2-3KDS (C) and decreased L-alanine (3,3,3)-D3 incorporation into D3-d3KDS (D) in the *tsc3Δ* mutant. WT and *tsc3Δ* yeasts were cultured in SD medium to the log phase. L-Serine (3,3)-D2 or L-alanine (3,3,3)-D3 was added to the culture at 7.6 mM. Approximately 2–4 × 10^8 of the cells were collected at the indicated time points for lipid extraction and LCB quantification by HPLC-ESI-MS/MS. Also shown are the incorporation of deuterated serine or alanine into *orm1Δorm2Δ* and *orm1Δorm2Δtsc3Δ* mutant yeast.

by lipid analysis of cells collected at different time points in WT and *tsc3Δ* (Fig. 3C, D). The incorporation of L-serine (3,3)-D2 into D2-3KDS was detected as early as 15 min after the addition of the label to the WT culture. Fig. 3C shows an ~4-fold faster rate of D2-3KDS formation in *tsc3Δ* than WT. The fastest rate of incorporation of L-serine (3,3)-D2 into D2-3KDS for WT occurred at ~60–90 min, with a rate of ~0.07 pmol D2-3KDS generated per minute per OD of cells. The *tsc3Δ* mutant showed a rate of ~0.23 pmol D2-3KDS generated per minute per OD of cells at 30–60 min. In contrast to the increased utilization of L-serine (3,3)-D2 by SPT, Fig. 3D shows a profound decrease of the incorporation of L-alanine (3,3,3)-D3 into D3-d3KDS in *tsc3Δ* cells, where D3-d3KDS was below the linear detection range for the 0–180 min time period used for the labeling assay. The formation of D3-d3KDS in WT started to be detected at ~90 min, which is later than the incorporation of L-serine (3,3)-D2 into 3KDS. The incorporation rate was at ~0.0023 pmol D3-d3KDS generated per minute per OD of cells, which is ~30-fold slower than the rate of serine incorporation into 3KDS. From these results, we conclude that *1*) knockout *TSC3* has opposite effects on serine and alanine utilization by SPT and causes decreased alanine and increased serine incorporation into the SPL synthesis pathway, and *2*) yeast cells utilize serine and alanine differently, with alanine incorporation into the SPL pathway at a much slower rate than serine. The *orm1Δ orm2Δ* mutant yeast were also included in this labeling assay with deuterated serine or alanine. The incorporation of both L-serine (3,3)-D2 and L-alanine (3,3,3)-D3 into 3KDS was dramatically increased compared with WT, confirming the role of Orm1/2 as general inhibitors of SPT toward both serine and alanine. Moreover, the deletion of TSC3 had a minor effect on the increased serine incorporation into 3KDS in *orm1Δ orm2Δ* but completely abolished the alanine incorporation into d3KDS. The results from the deuterated serine or alanine labeling assay in *orm1Δ orm2Δ tsc3Δ* mutant yeast show that Tsc3 is indispensable for the increased alanine incorporation into SPLs in *orm1Δ omr2Δ* but only partially required for the increased serine incorporation into the *orm1Δ omr2Δ* mutant.

To investigate how Tsc3 controls SPT amino acid selectivity, SPT in vitro assays using microsomes from either WT or *tsc3Δ* cells were performed to assess SPT activity directly with L-serine (3,3)-D2 or L-alanine (3,3,3)-D3 as substrates. Although the existence of deoxy-LCBs is evident in yeast lipid extracts and alanine incorporation into the SPL pathway is clearly detected in the in vivo labeling assay with L-alanine (3,3,3)-D3, no deuterated d3KDS was detected for the in vitro SPT assay with L-alanine (3,3,3)-D3 as a substrate. This suggests that the in vitro system with microsomes as the SPT source somehow does not fully recapitulate in vivo SPT activity. This is possibly due to the impairment of the oligomerization of the SPT complex or the loss of factors required for alanine incorporation during the microsome purification process. On the other hand, WT microsomes showed robust SPT activity toward serine measured by the incorporation of L-serine (3,3)-D2 into D2-3KDS (**Fig. 4A**). Tsc3 was reported as an activator of SPT because the in vitro SPT activity was greatly reduced in the *tsc3Δ* (by ~30-fold) shown by the in vitro SPT assay with radiolabeled serine as a substrate (6). We also saw this severe reduction of SPT activity when using microsomes prepared from *tsc3Δ* cultured at 30°C. Later we found out that

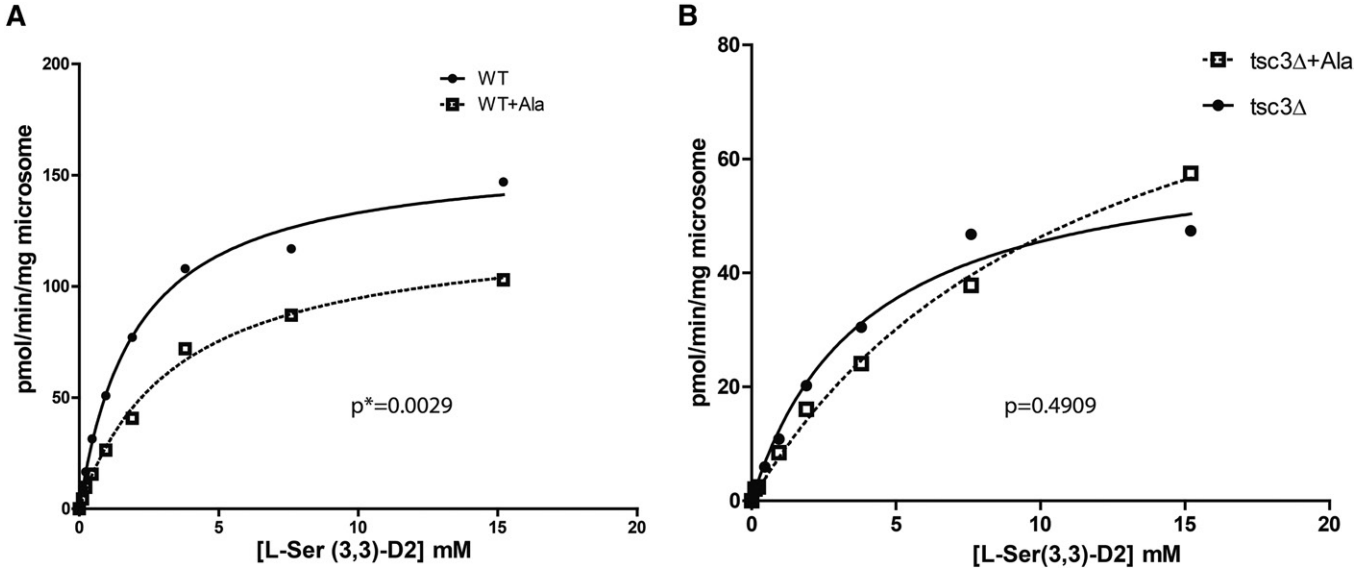

Fig. 4. Tsc3 is required for alanine inhibition of serine incorporation into 3KDS by SPT. In vitro SPT activity assay with L-serine as a substrate using WT (A) and tsc3Δ microsomes (B) in the presence (dotted line) or absence of 7.6 mM alanine (solid line). SPT kinetics toward serine were measured by plotting the initial velocity of the reaction (the amount of D2-3KDS generated per microgram of microsomes per minute) against L-serine (3,3)-D2 concentrations used in the reaction ranging from 0 to 15.2 mM. Microsomes (200 μg) and 100 μM palmitoyl-CoA were used in all reactions. The data were fitted using the Michaelis-Menten equation and generated using GraphPad Prism 5. In the absence of alanine, the WT microsome SPT K_m value for serine was 2.0 ± 0.4 mM, and V_{max} was 160.0 ± 10.8 pmol/min/mg yeast microsome. In the presence of alanine, K_m for serine was 3.4 ± 0.6 mM, and V_{max} was 127.4 ± 9.4 pmol/min/mg yeast microsome. *P* values from the paired *t*-test comparing SPT velocity in the presence or absence of alanine are shown. *Significant difference between two groups of data.

30°C is not the optimal culture condition because *tsc3Δ* cells died rapidly with the increase of temperature. A fraction of cell death was detected when *tsc3Δ* cells were cultured at 30°C, and complete cell death occurred at 37°C. Thus, we cultured cells at 24°C, a temperature at which no cell death occurred, and cells grew at the similar rate as WT cells in SD medium. The in vitro SPT assay was also performed at 24°C. Under this condition, SPT activity toward serine from *tsc3Δ* microsome fractions was comparable to WT, although it was still ∼2–5-fold lower (Fig. 4B). The possibly less stable SPT complex caused by *TSC3* knockout, which could be worsened by the microsome purification process, might be the reason for the decreased in vitro SPT activity in *tsc3Δ* microsome fractions. Nonetheless, no increased in vitro SPT activity toward serine from *tsc3Δ* microsomes was observed. This suggests that the increased serine incorporation into 3KDS in *tsc3Δ* cell culture is not due to increases in SPT catalytic activity toward serine.

That no production of d3KDS was detected for the SPT in vitro assay with alanine as a substrate under the same condition in which SPT showed robust activity toward serine suggests a dramatic difference between SPT dynamics toward the two amino acid substrates. This is consistent with the in vivo labeling assay with deuterated L-serine or L-alanine as shown in Fig. 3 in that the incorporation of serine was much faster than that of alanine. Another way to study in vitro SPT activity toward alanine is to evaluate its ability to compete with serine for SPT activity. SPT kinetics in response to different concentrations of L-serine (3,3)-D2 were measured in the presence of 7.6 mM alanine (Fig. 4A). The addition of alanine decreased SPT activity toward L-serine (3,3)-D2 at all of the serine concentrations tested. Kinetic analysis showed increased K_m and decreased V_{max} for SPT catalytic activity toward serine in the presence of alanine. These data demonstrate that alanine is a potent inhibitor for SPT activity toward serine, most likely through direct competition with serine. It is important to note that this alanine inhibition of serine incorporation into 3KDS by SPT was abolished when microsome fractions from *tsc3Δ* were used for the in vitro SPT assay (Fig. 4B).

Together, these results show that Tsc3 is required for efficient SPT utilization of alanine and its inhibition of SPT-catalyzed serine incorporation into 3KDS. The increase in serine incorporation into 3KDS in *tsc3Δ* demonstrated by the in vivo labeling assay was caused by the lack of alanine inhibition on SPT activity toward serine but not increased SPT catalytic activity toward serine from the *tsc3Δ* microsome. At this point, we cannot exclude the possibility that the increased in vivo SPT activity toward serine in *tsc3Δ* was also due to posttranslational modifications, which can only be preserved in intact cells.

Increased CerS activity in *tsc3Δ* cells

Although the L-serine (3,3)-D2 labeling assay showed a clear increase in serine incorporation into SPLs in *tsc3Δ* cells measured by the faster formation of 3KDS at all conditions tested, we also consistently observed decreased PHS levels and occasionally decreased DHS levels in this mutant when measuring the steady-state lipid level under various culture conditions (Fig. 2A, F). This might have been caused by a decrease in PHS production from DHS catalyzed by the sphinganine C4-hydroxylase, Sur2, or by an increase in the conversion from PHS/DHS to PHC/DHC with the yeast CerSs Lag1/Lac1 and Lip1. To test this, levels of ceramides were first measured in WT and *tsc3Δ* yeast cultured in SD medium to the late-log phase. DHC and PHC with the C26 acyl chain, DHC (d18:0/26:0) and PHC (d18:0/26:0), are the major ceramide species in yeast, and they are both generated by yeast CerS with DHS or PHS as substrates, respectively. Increased accumulation of both DHC (d18:0/26:0) and PHC (d18:0/26:0) was observed in *tsc3Δ* cells (**Fig. 5A**). To show that the lack of *TSC3* is responsible for ceramide accumulation in *tsc3Δ*, lipid analysis was performed in WT, *tsc3Δ*, and *tsc3Δ* transformed with the WT *TSC3* gene. Again, the results showed accumulation of DHC (d18:0/26:0) in *tsc3Δ* cells and was brought back to the WT level when *TSC3* was introduced back to the strain (Fig. 5B). The accumulation of PHC (d18:0/26:0) in *tsc3Δ* containing the vector control was not obvious under this culture condition.

To determine whether the accumulation of ceramides in *tsc3Δ* cells shown by the steady-state measurement of bulk lipid was due to increased ceramide synthesis in *tsc3Δ* cells, we developed a labeling assay with the addition of C17-DHS (DHS [d17:0]) to the culture medium and monitored its incorporation into C17-DHC (d17:0/26:0), C17-PHS, and C17-PHC (d17:0/26:0). The results showed that there was a dramatic increase in the formation of C17-DHC (d17:0/26:0) in *tsc3Δ* cells compared with WT (Fig. 5C). A large increase in the production of C17-PHC (d17:0/26:0) was also observed in *tsc3Δ* cells (Fig. 5E). On the other hand, the generation of C17-PHS from C17-DHS was comparable between WT and *tsc3Δ*, with a slight decrease at later time points in *tsc3Δ*. These results show increased CerS activity in *tsc3Δ* but no change in hydroxylase activity.

Next, in vitro assays to measure CerS activity were performed with either WT or *tsc3Δ* microsome fractions as the enzyme source and C17-DHS and palmitoyl-CoA as substrates (data not shown). No major difference was seen between in vitro CerS activity of WT and *tsc3Δ* cells, suggesting the upregulation of CerS activity in *tsc3Δ* cells requires an intact cellular context, possibly through posttranslational regulation.

Ypk1 is required for increased serine flux into SPL synthesis in *tsc3Δ* by activating both SPT and CerS

The above results demonstrate increased ceramide synthesis in *tsc3Δ* cells by the in vivo labeling assay with C17-DHS, suggesting the operation of a regulatory response downstream of the effects of Tsc3 on SPT. Ypk1 is a yeast homologue of human serum- and glucocorticoid-induced kinase. It is a serine/threonine kinase that belongs to the ACG kinase family and controls various downstream cellular processes through phosphorylation of different target proteins (32). Ypk1 is activated by target of rapamycin complex 2 (TORC2) and Pkh1/2, the yeast homologues of mammalian phosphoinositide-dependent protein kinase 1.

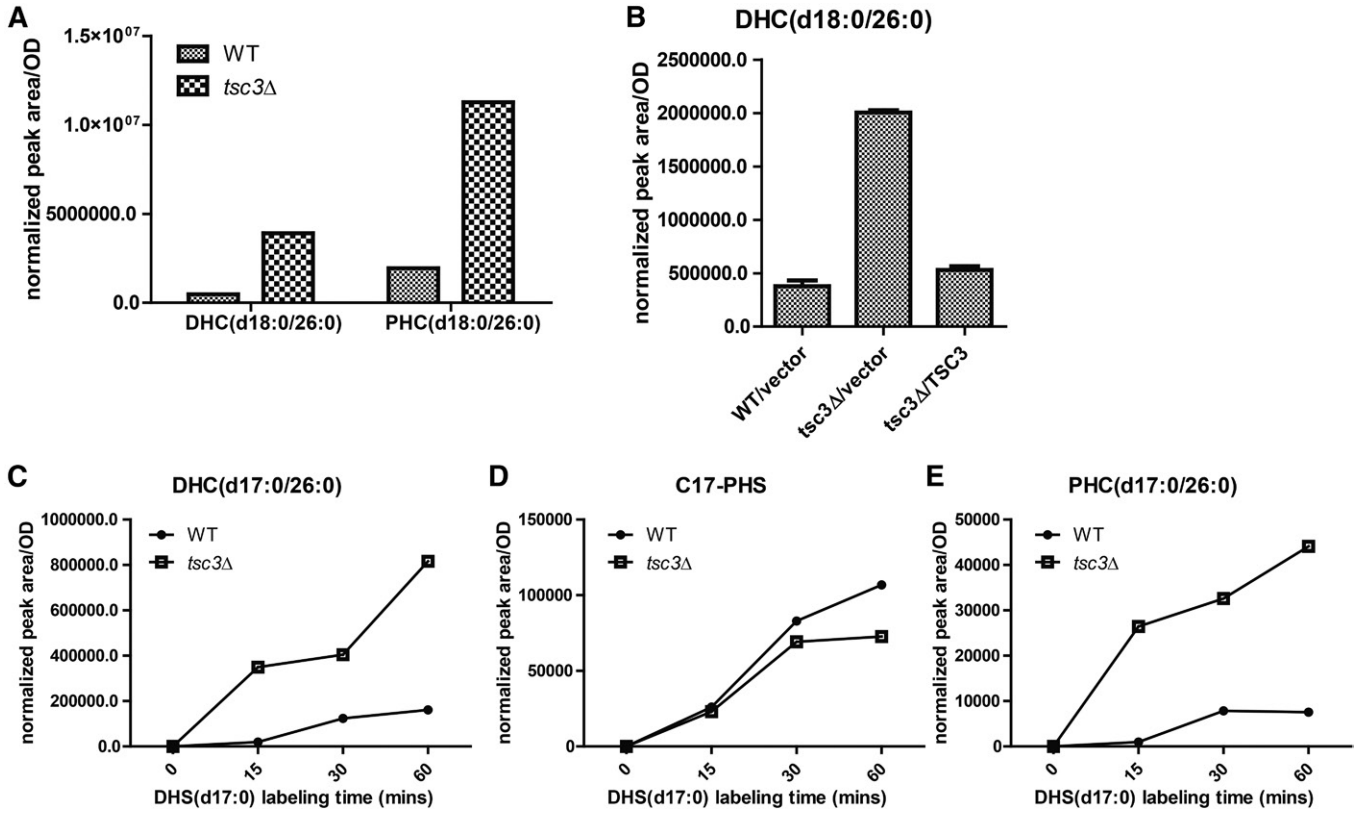

Fig. 5. Increased CerS activity in *tsc3Δ*. A: Accumulation of DHC (d18:0/26:0) and PHC (d18:0/26:0) in *tsc3Δ*. WT and *tsc3Δ* were cultured in SD medium to the late-log phase before lipid extraction and HPLC-ESI-MS/MS quantification of indicated ceramide species. The result shown is one representative from at least three independent experiments. B: The accumulation of DHC (d18:0/26:0) in *tsc3Δ* is reversed by introducing the WT *TSC3* gene in the knockout strain. The indicated strains were cultured in SD-leucine medium to the late-log phase before lipid extraction and HPLC-ESI-MS/MS quantification of indicated ceramide species. Increased incorporation of C17-DHS into DHC (d17:0/26:0) (C) and PHC (d17:0/26:0) (E). C17-DHS was converted to C17-PHS at similar rate between WT and *tsc3Δ* (D). WT and *tsc3Δ* cells were cultured in SD medium to the log phase before the addition of 10 μM C17-DHS. Cells were collected at the indicated time points for lipid analysis.

TORC2-dependent activation of Ypk1 promotes de novo SPL biosynthesis through the phosphorylation of two known Ypk1 targets, Orm1/2 and Lag1/Lac1 (12, 33–35). The phosphorylation of Orm1/2 relieves its repression of SPT activity and thus promotes serine influx in the SPL pathway. The phosphorylation of the yeast CerS catalytic subunit Lag1/Lac1 upregulates its activity and promotes ceramide synthesis.

To test whether Ypk1 is involved in the activation of CerS in *tsc3Δ* cells, we measured CerS activity in *tsc3Δypk1Δ* double-knockout cells using the in vivo labeling assay with C17-DHS (**Fig. 6A–**D). Eliminating Ypk1 from *tsc3Δ* cells abolished the increased C17-DHS incorporation into the C17-DHC and C17-PHC shown in *tsc3Δ* cells. On the other hand, the deletion of Ypk2, the Ypk1 paralogue, showed no such effect. Neither the deletion of Pkh1 nor Pkh2, the serine/threonine kinase kinases that are required for the basal activation of Ypk1, affected the increased CerS activity in *tsc3Δ* cells, possibly due to their redundant activity. These data show that Ypk1 is specifically required for increased CerS activity in *tsc3Δ* cells.

Although Fig. 4 shows that the increased incorporation of L-serine into 3KDS in *tsc3Δ* culture is due to a lack of alanine inhibition, we cannot exclude the possibility that SPT is also activated/derepressed in vivo, especially considering Orm1/2 are Ypk1 substrates and their phosphorylation by Ypk1 leads to SPT depression. To determine whether the in vivo SPT activity is derepressed by Ypk1 in *tsc3Δ* cells, the incorporation of L-serine (3,3)-D2 into D2-3KDS was monitored in WT, *tsc3Δ*, and *tsc3Δypk1Δ* cells (Fig. 6E). The deletion of YPK1 decreased serine incorporation into 3KDS in *tsc3Δ* cells, showing Ypk1-mediated SPT derepression contributes to increased serine incorporation into 3KDS in *tsc3Δ*. Fig. 6E also shows that although the rate of serine incorporation into 3KDS in the *tsc3Δypk1Δ* double mutant was slower than *tsc3Δ*, it was still higher than WT, suggesting Ypk1 is only partially responsible for the increased L-serine incorporation into 3KDS observed in *tsc3Δ*. We thus attribute the increase in serine incorporation into 3KDS from WT to *tsc3Δypk1Δ* to the lack of L-alanine inhibition. With this experiment, we conclude that both the lack of inhibition from alanine in the SPT reaction as well as the Ypk1-mediated SPT derepression through Orm1/2 inactivation contribute to the increased serine influx into the SPL pathway in *tsc3Δ* cells.

These results strongly suggest the activation of the Ypk1-signaling pathway in response to *TSC3* knockout. This activation of Ypk1 signaling is downstream of the imbalance between serine and alanine incorporation into SPLs caused by the *TSC3* deletion. This is demonstrated by the

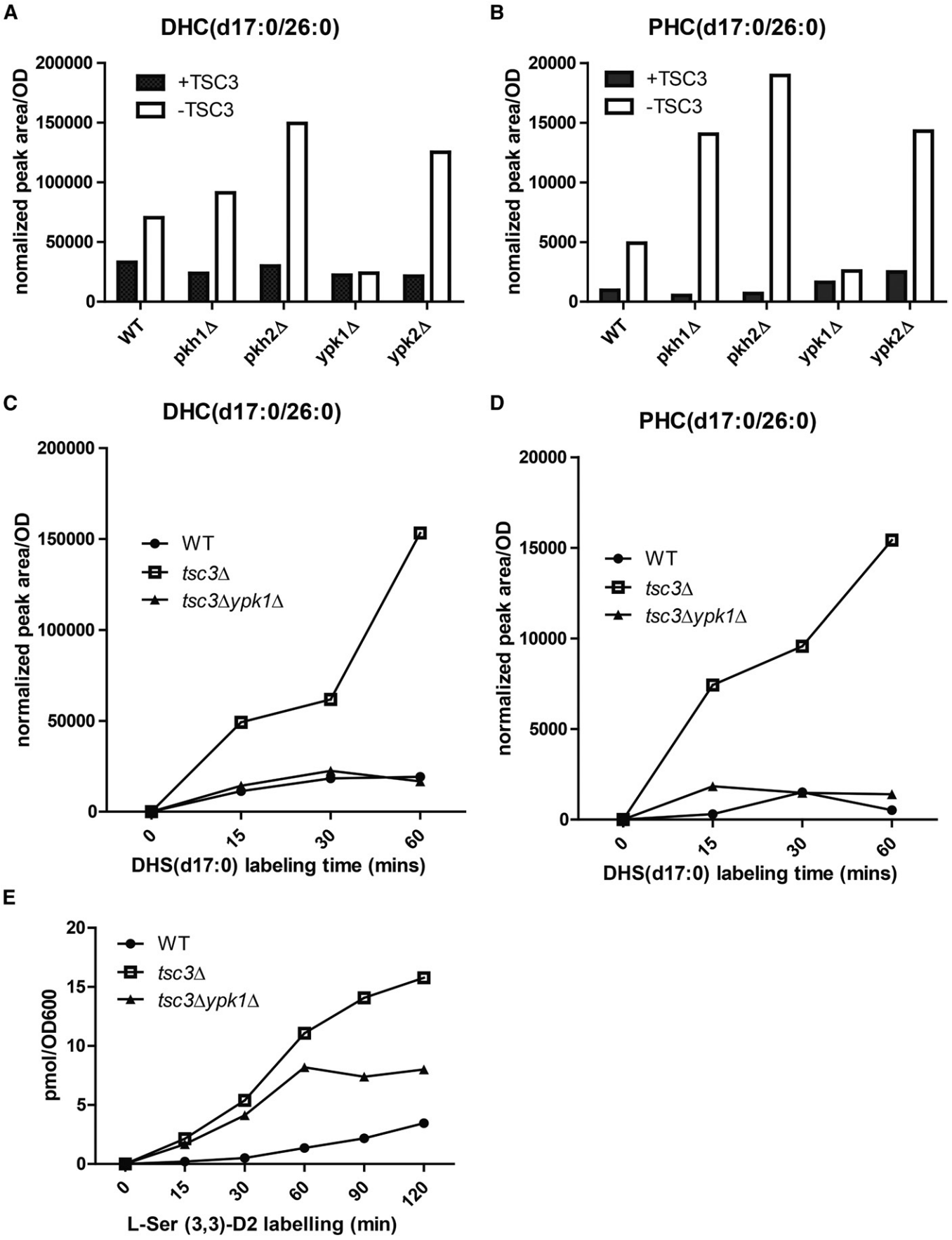

Fig. 6. Ypk1 is required for the activation of CerS and SPT in *tsc3Δ*. A–D: The increased formation of C17-DHC and C17-PHC from C17-DHS labeling in *tsc3Δ* is Ypk1-depenedent. A, B: WT and indicated mutant yeast strains were cultured to the late-log phase in SD medium

observation that the incorporation of both serine and alanine into SPL in *ypk1Δ* is at a similar rate as WT (data not shown).

DISCUSSION

Through a detailed characterization of SPL profiles of *tsc3Δ* with the ability to distinguish between serine and alanine derivatives, we have shown that the primary function of Tsc3 is to promote alanine incorporation into the SPL pathway through SPT utilization (**Fig. 7**). The loss of Tsc3 causes greatly decreased utilization of alanine and relieves the inhibitory effect of alanine on serine utilization by SPT, which results in increased serine influx into the SPL pathway. The influx of serine into the SPL pathway is further promoted by the activation of both SPT and CerS in a Ypk1-dependent manner. In summary, this study shows SPT can utilize both serine and alanine to generate canonical and noncanonical SPLs with the serine influx at a faster rate than alanine influx. Canonical SPLs become the even more dominant species in response to *TSC3* knockout, with an increased serine influx and greatly decreased alanine influx into the SPL pathway.

In this study, we defined the primary role of Tsc3 as a regulator in SPT amino acid selectivity and stated that it is required for the efficient utilization of alanine by SPT. Tsc3 has been suggested as an SPT activator mainly from in vitro assays that showed greatly reduced SPT activity in *tsc3Δ*. In vitro SPT assays using purified microsomes from various organisms have been intensively used to study SPT activity. However, the in vitro assay does have some limitations, as shown in this study. First, alanine incorporation into SPLs was not observable even when using microsomes from WT; thus, the in vitro assay does not fully recapitulate the in vivo system. Second, the integrity of the SPT complex might be hard to preserve when microsome fractions are used, especially when one or more subunits are missing. Third, the in vitro SPT activity may not reflect the effects of posttranslational modifications and/or allosteric regulation because many of them can be transient in nature and difficult to conserve with the in vitro system. The in vivo labeling assay using deuterated amino acid substrates to monitor the formation of SPT products directly using the HPLC-ESI-MS/MS method developed in this study solved the three aforementioned problems. In addition, the separation and quantification of free LCBs with the HPLC-ESI-MS/MS method established with the specifically synthesized standard compounds shows great sensitivity and specificity and allowed us to measure the small quantity of free LCBs directly generated from SPT instead of measuring total LCBs, including both free LCBs and the LCB moieties released from ceramide and complex SPLs with base and acid hydrolysis, which has been used often to evaluate serine- versus alanine-based SPLs. However, the level of total LCBs shows the cumulative effect of all the metabolic enzymes in the SPL pathway and does not necessarily exclusively reflect SPT activity. Moreover, this approach also provides an important complement to the analysis of the steady-state SPL measurement. This is demonstrated by the fact that although the steady level of the major serine-derived LCB, PHS, was greatly reduced in the *tsc3Δ* mutant, it does not necessarily suggest a decreased serine influx. With the labeling assay using L-serine (3,3)-D2 to monitor SPT activity and C17-DHS to monitor CerS activity, the results showed that this decreased steady-state level of PHS is actually caused by a faster conversion of PHS into PHC, although the incorporation of serine into 3KDS is actually increased in *tsc3Δ*. In summary, this in vivo labeling assay is critical in revealing the difference in the formation of 3KDS and d3KDS from serine and alanine through SPT between WT and *tsc3Δ*. It also helps to discover that in contrast to Tsc3, which has the opposite effect on alanine and serine utilization by SPT, Orm1/2 are negative regulators of SPT and inhibit the formation of both LCBs and deoxy-LCBs.

Compared with the mechanism of SPT activity toward serine, there is little known about SPT activity on alanine. One major reason is that no SPT activity is detected toward alanine with the in vitro SPT assay, as demonstrated by this study and others (21). The in vivo labeling assay with deuterated serine or alanine used in this study showed different dynamics for SPT utilization of the two amino acid substrates with a much slower incorporation rate for alanine, which also occurred at a later cell growth stage compared with SPT utilization of serine. These results confirm that serine is the preferred SPT substrate. However, the regulatory mechanism of SPT substrate selectivity is still not clear. This study further demonstrates that Tsc3 is required for efficient alanine incorporation into SPL. It is possible that cells regulate this difference in the utilization of serine versus alanine by SPT by adjusting *TSC3* gene expression either at the transcription or posttranslational modification level.

This study also provides some structural insights into the catalytic mechanism of SPT toward serine and alanine. The proposed pyridoxl 5′-phosphate-dependent SPT catalytic mechanism suggests that serine and alanine most likely share the same SPT binding and catalytic mechanism (36–41). This determines their competitive nature for their utilization by SPT. In this study, we showed that alanine indeed was able to inhibit the utilization of serine by SPT, and this inhibitory effect depended on the existence of Tsc3 in the SPT complex. This suggests that the yeast SPT complex without the Tsc3 subunit is not readily accessible to alanine. Thus, our study provides a possible regulatory mechanism that controls SPT substrate selectivity through changes in amino acid substrate accessibility to the enzyme, most likely by conformational changes.

---

and labeled with C17-DHS for 30 min. Lipids were extracted and subjected to HPLC-ESI-MS/MS to detect C17-DHC (A) and C17-PHC (B). Their relative amount was normalized by an internal standard and the amount of cells used (OD) as shown on the *y*-axis. The result shown is one representative from at least three independent experiments. C, D: WT, *tsc3Δ*, and *tsc3Δ ypk1Δ* were cultured to the log phase and labeled with 10 μM C17-DHS for the indicated time. The relative amount of C17-DHC (C) or C17-PHS (D) generated was plotted against labeling time. E: WT, *tsc3Δ*, and *tsc3Δ ypk1Δ* were cultured to the log phase and labeled with 7.6 mM L-serine (3,3)-D2 for the indicated time. The amount of D2-3KDS generated was plotted against the time points.

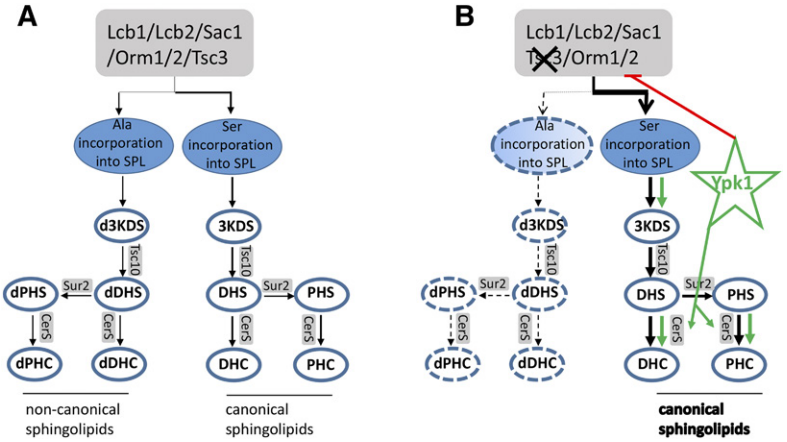

Fig. 7. Tsc3 regulates the balance between canonical and noncanonical SPLs by promoting L-alanine incorporation into the SPL de novo synthesis pathway. A: Both alanine and serine are utilized by the intact SPT complex to maintain a homeostasis between canonical and noncanonical SPLs. Serine influx into canonical SPLs is at a faster rate than alanine incorporation into noncanonical SPLs. B: Eliminating the Tsc3 subunit from the SPT complex changes SPL homeostasis, with the generation of canonical SPLs becoming more dominant. The increased serine influx in *tsc3Δ* is partially due to the lack of alanine inhibition. The serine influx is also further boosted with Ypk1-dependent SPT derepression through Om1/2 deactivation and Ypk1-depenent CerS activation. The production of complex SPLs is not shown in these schemes. Enzymes in the SPL pathway are shown in gray boxes. SPL intermediate metabolites are shown in ovals with a blue outline. Ypk1's action on its substrates are indicated with a red line (inhibition) and green arrow (activation). Steps of Ypk1-depdent increases in serine influx into the SPL pathway are shown with bold green arrows.

These results support and extend regulatory roles for the kinase Ypk1 in regulating SPL metabolism. The CerS catalytic subunits Lac1/lag1 and SPT subunits Orm1/2 are known Ypk1 substrates (34, 42), and Ypk1 is generally believed to be activated through the TORC2 pathway in response to membrane stress, such as caused by myriocin treatment or heat stress, to promote serine influx into the SPL pathway (9, 33, 34, 42). Although compromised SPL synthesis was suggested as triggering the activation of Ypk1, the exact signal that directly causes Ypk1 activation is not known. Our study shows the Ypk1-dependent activation of both SPT and CerS as an important effect in *tsc3Δ* cells downstream of imbalanced alanine and serine utilization by SPT. At this stage, we cannot pinpoint which specific lipid changes, the decrease in alanine or increased serine influx into the SPL pathway, causes the downstream activation of Ypk1 signaling. Considering the activation of Ypk1 signaling in response to myriocin treatment, the results favor that compromised deoxy-SPL synthesis is possibly the primary signal that activates Ypk1 signaling to promote serine influx into the SPL pathway. Enlightened by this study we plan to test the hypothesis that deoxy-SPLs affect Ypk1 signaling either through the TORC2 or Pkh1/2 pathway. We believe this study provides a glimpse of the possible physiologic function of deoxy-SPLs, and future endeavors will contribute significantly to the understanding of the cellular role of deoxy-SPLs and thus the pathophysiology associated with HSAN1.

REFERENCES

1. Hannun, Y. A., and L. M. Obeid. 2018. Sphingolipids and their metabolism in physiology and disease. *Nat. Rev. Mol. Cell Biol.* **19:** 175–191.
2. Dickson, R. C., and R. L. Lester. 1999. Yeast sphingolipids. *Biochim. Biophys. Acta.* **1426:** 347–357.
3. Lowther, J., J. H. Naismith, T. M. Dunn, and D. J. Campopiano. 2012. Structural, mechanistic and regulatory studies of serine palmitoyltransferase. *Biochem. Soc. Trans.* **40:** 547–554.
4. Nagiec, M. M., J. A. Baltisberger, G. B. Wells, R. L. Lester, and R. C. Dickson. 1994. The LCB2 gene of Saccharomyces and the related LCB1 gene encode subunits of serine palmitoyltransferase, the initial enzyme in sphingolipid synthesis. *Proc. Natl. Acad. Sci. USA.* **91:** 7899–7902.
5. Hanada, K., T. Hara, M. Nishijima, O. Kuge, R. C. Dickson, and M. M. Nagiec. 1997. A mammalian homolog of the yeast LCB1 encodes a component of serine palmitoyltransferase, the enzyme catalyzing the first step in sphingolipid synthesis. *J. Biol. Chem.* **272:** 32108–32114.
6. Gable, K., H. Slife, D. Bacikova, E. Monaghan, and T. M. Dunn. 2000. Tsc3p is an 80-amino acid protein associated with serine palmitoyltransferase and required for optimal enzyme activity. *J. Biol. Chem.* **275:** 7597–7603.
7. Han, G., S. D. Gupta, K. Gable, S. Niranjanakumari, P. Moitra, F. Eichler, R. H. Brown, Jr., J. M. Harmon, and T. M. Dunn. 2009. Identification of small subunits of mammalian serine palmitoyltransferase that confer distinct acyl-CoA substrate specificities. *Proc. Natl. Acad. Sci. USA.* **106:** 8186–8191.
8. Han, S., M. A. Lone, R. Schneiter, and A. Chang. 2010. Orm1 and Orm2 are conserved endoplasmic reticulum membrane proteins regulating lipid homeostasis and protein quality control. *Proc. Natl. Acad. Sci. USA.* **107:** 5851–5856.
9. Breslow, D. K., S. R. Collins, B. Bodenmiller, R. Aebersold, K. Simons, A. Shevchenko, C. S. Ejsing, and J. S. Weissman. 2010. Orm family proteins mediate sphingolipid homeostasis. *Nature.* **463:** 1048–1053.
10. Pinto, W. J., G. W. Wells, and R. L. Lester. 1992. Characterization of enzymatic synthesis of sphingolipid long-chain bases in Saccharomyces cerevisiae: mutant strains exhibiting long-chain-base auxotrophy are deficient in serine palmitoyltransferase activity. *J. Bacteriol.* **174:** 2575–2581.
11. Russo, S. B., R. Tidhar, A. H. Futerman, and L. A. Cowart. 2013. Myristate-derived d16:0 sphingolipids constitute a cardiac sphingolipid pool with distinct synthetic routes and functional properties. *J. Biol. Chem.* **288:** 13397–13409.
12. Rosenberg, A., and N. Stern. 1966. Changes in sphingosine and fatty acid components of the gangliosides in developing rat and human brain. *J. Lipid Res.* **7:** 122–131.
13. Sonnino, S., and V. Chigorno. 2000. Ganglioside molecular species containing C18- and C20-sphingosine in mammalian nervous tissues and neuronal cell cultures. *Biochim. Biophys. Acta.* **1469:** 63–77.

14. Hornemann, T., A. Penno, M. F. Rutti, D. Ernst, F. Kivrak-Pfiffner, L. Rohrer, and A. von Eckardstein. 2009. The SPTLC3 subunit of serine palmitoyltransferase generates short chain sphingoid bases. *J. Biol. Chem.* **284:** 26322–26330.
15. Zhao, L., S. Spassieva, K. Gable, S. D. Gupta, L. Y. Shi, J. Wang, J. Bielawski, W. L. Hicks, M. P. Krebs, J. Naggert, et al. 2015. Elevation of 20-carbon long chain bases due to a mutation in serine palmitoyltransferase small subunit b results in neurodegeneration. *Proc. Natl. Acad. Sci. USA.* **112:** 12962–12967.
16. Pruett, S. T., A. Bushnev, K. Hagedorn, M. Adiga, C. A. Haynes, M. C. Sullards, D. C. Liotta, and A. H. Merrill, Jr. 2008. Biodiversity of sphingoid bases ("sphingosines") and related amino alcohols. *J. Lipid Res.* **49:** 1621–1639.
17. Zitomer, N. C., T. Mitchell, K. A. Voss, G. S. Bondy, S. T. Pruett, E. C. Garnier-Amblard, L. S. Liebeskind, H. Park, E. Wang, M. C. Sullards, et al. 2009. Ceramide synthase inhibition by fumonisin B1 causes accumulation of 1-deoxysphinganine: a novel category of bioactive 1-deoxysphingoid bases and 1-deoxydihydroceramides biosynthesized by mammalian cell lines and animals. *J. Biol. Chem.* **284:** 4786–4795.
18. Bejaoui, K., C. Wu, M. D. Scheffler, G. Haan, P. Ashby, L. Wu, P. de Jong, and R. H. Brown, Jr. 2001. SPTLC1 is mutated in hereditary sensory neuropathy, type 1. *Nat. Genet.* **27:** 261–262.
19. Dawkins, J. L., D. J. Hulme, S. B. Brahmbhatt, M. Auer-Grumbach, and G. A. Nicholson. 2001. Mutations in SPTLC1, encoding serine palmitoyltransferase, long chain base subunit-1, cause hereditary sensory neuropathy type I. *Nat. Genet.* **27:** 309–312.
20. Rotthier, A., M. Auer-Grumbach, K. Janssens, J. Baets, A. Penno, L. Almeida-Souza, K. Van Hoof, A. Jacobs, E. De Vriendt, B. Schlotter-Weigel, et al. 2010. Mutations in the SPTLC2 subunit of serine palmitoyltransferase cause hereditary sensory and autonomic neuropathy type I. *Am. J. Hum. Genet.* **87:** 513–522.
21. Gable, K., S. D. Gupta, G. Han, S. Niranjanakumari, J. M. Harmon, and T. M. Dunn. 2010. A disease-causing mutation in the active site of serine palmitoyltransferase causes catalytic promiscuity. *J. Biol. Chem.* **285:** 22846–22852.
22. Penno, A., M. M. Reilly, H. Houlden, M. Laura, K. Rentsch, V. Niederkofler, E. T. Stoeckli, G. Nicholson, F. Eichler, R. H. Brown, Jr., et al. 2010. Hereditary sensory neuropathy type 1 is caused by the accumulation of two neurotoxic sphingolipids. *J. Biol. Chem.* **285:** 11178–11187.
23. Bode, H., F. Bourquin, S. Suriyanarayanan, Y. Wei, I. Alecu, A. Othman, A. Von Eckardstein, and T. Hornemann. 2016. HSAN1 mutations in serine palmitoyltransferase reveal a close structure-function-phenotype relationship. *Hum. Mol. Genet.* **25:** 853–865.
24. Longtine, M. S., A. McKenzie III, D. J. Demarini, N. G. Shah, A. Wach, A. Brachat, P. Philippsen, and J. R. Pringle. 1998. Additional modules for versatile and economical PCR-based gene deletion and modification in Saccharomyces cerevisiae. *Yeast.* **14:** 953–961.
25. Gueldener, U., J. Heinisch, G. J. Koehler, D. Voss, and J. H. Hegemann. 2002. A second set of loxP marker cassettes for Cre-mediated multiple gene knockouts in budding yeast. *Nucleic Acids Res.* **30:** e23.
26. Ren, J., J. Snider, M. V. Airola, A. Zhong, N. A. Rana, L. M. Obeid, and Y. A. Hannun. 2018. Quantification of 3-ketodihydrosphingosine using HPLC-ESI-MS/MS to study SPT activity in yeast *Saccharomyces cerevisiae. J Lipid Res.* **59:** 162–170.
27. Snider, J. M., A. J. Snider, L. M. Obeid, C. Luberto, and Y. A. Hannun. 2018. Probing de novo sphingolipid metabolism in mammalian cells utilizing mass spectrometry. *J. Lipid Res.* **59:** 1046–1057.
28. Beeler, T., D. Bacikova, K. Gable, L. Hopkins, C. Johnson, H. Slife, and T. Dunn. 1998. The Saccharomyces cerevisiae TSC10/YBR265w gene encoding 3-ketosphinganine reductase is identified in a screen for temperature-sensitive suppressors of the Ca2+-sensitive csg2Delta mutant. *J. Biol. Chem.* **273:** 30688–30694.
29. Grilley, M. M., S. D. Stock, R. C. Dickson, R. L. Lester, and J. Y. Takemoto. 1998. Syringomycin action gene SYR2 is essential for sphingolipid 4-hydroxylation in Saccharomyces cerevisiae. *J. Biol. Chem.* **273:** 11062–11068.
30. Cuadros, R., E. Montejo de Garcini, F. Wandosell, G. Faircloth, J. M. Fernandez-Sousa, and J. Avila. 2000. The marine compound spisulosine, an inhibitor of cell proliferation, promotes the disassembly of actin stress fibers. *Cancer Lett.* **152:** 23–29.
31. Uhlig, S., D. Petersen, A. Flaoyen, and A. Wilkins. 2005. 2-Amino-14,16-dimethyloctadecan-3-ol, a new sphingosine analogue toxin in the fungal genus Fusarium. *Toxicon.* **46:** 513–522.
32. Pearce, L. R., D. Komander, and D. R. Alessi. 2010. The nuts and bolts of AGC protein kinases. *Nat. Rev. Mol. Cell Biol.* **11:** 9–22.
33. Berchtold, D., M. Piccolis, N. Chiaruttini, I. Riezman, H. Riezman, A. Roux, T. C. Walther, and R. Loewith. 2012. Plasma membrane stress induces relocalization of Slm proteins and activation of TORC2 to promote sphingolipid synthesis. *Nat. Cell Biol.* **14:** 542–547.
34. Muir, A., S. Ramachandran, F. M. Roelants, G. Timmons, and J. Thorner. 2014. TORC2-dependent protein kinase Ypk1 phosphorylates ceramide synthase to stimulate synthesis of complex sphingolipids. *eLife.* **3:** e03779.
35. Niles, B. J., and T. Powers. 2012. Plasma membrane proteins Slm1 and Slm2 mediate activation of the AGC kinase Ypk1 by TORC2 and sphingolipids in S. cerevisiae. *Cell Cycle.* **11:** 3745–3749.
36. Alexeev, D., R. L. Baxter, D. J. Campopiano, O. Kerbarh, L. Sawyer, N. Tomczyk, R. Watt, and S. P. Webster. 2006. Suicide inhibition of alpha-oxamine synthases: structures of the covalent adducts of 8-amino-7-oxononanoate synthase with trifluoroalanine. *Org. Biomol. Chem.* **4:** 1209–1212.
37. Hunter, G. A., and G. C. Ferreira. 1999. Lysine-313 of 5-aminolevulinate synthase acts as a general base during formation of the quinonoid reaction intermediates. *Biochemistry.* **38:** 3711–3718.
38. Ikushiro, H., M. M. Islam, A. Okamoto, J. Hoseki, T. Murakawa, S. Fujii, I. Miyahara, and H. Hayashi. 2009. Structural insights into the enzymatic mechanism of serine palmitoyltransferase from Sphingobacterium multivorum. *J. Biochem.* **146:** 549–562.
39. Kerbarh, O., D. J. Campopiano, and R. L. Baxter. 2006. Mechanism of alpha-oxoamine synthases: identification of the intermediate Claisen product in the 8-amino-7-oxononanoate synthase reaction. *Chem. Commun. (Camb.).* 60–62.
40. Raman, M. C., K. A. Johnson, B. A. Yard, J. Lowther, L. G. Carter, J. H. Naismith, and D. J. Campopiano. 2009. The external aldimine form of serine palmitoyltransferase: structural, kinetic, and spectroscopic analysis of the wild-type enzyme and HSAN1 mutant mimics. *J. Biol. Chem.* **284:** 17328–17339.
41. Webster, S. P., D. Alexeev, D. J. Campopiano, R. M. Watt, M. Alexeeva, L. Sawyer, and R. L. Baxter. 2000. Mechanism of 8-amino-7-oxononanoate synthase: spectroscopic, kinetic, and crystallographic studies. *Biochemistry.* **39:** 516–528.
42. Roelants, F. M., D. K. Breslow, A. Muir, J. S. Weissman, and J. Thorner. 2011. Protein kinase Ypk1 phosphorylates regulatory proteins Orm1 and Orm2 to control sphingolipid homeostasis in Saccharomyces cerevisiae. *Proc. Natl. Acad. Sci. USA.* **108:** 19222–19227.